MATERIAL FORMING SIMULATION ENVIRONMENT BASED ON QFORM3D SOFTWARE SYSTEM

Nikolay Biba[1], Sergey Stebunov[1], Alexey Vlasov[2]

[1] QuantorForm Ltd., Moscow, Russia
[2]Moscow State Industrial University, Moscow, Russia

ABSTRACT

The paper presents a new step in development of metal forming simulation software QForm3D towards creation a multi disciplinary simulation environment for the analysis of material forming technologies. For its development the object-oriented method and the most up-to-date programming technique are used. This provides enough flexibility for including in the software different methods and approaches depending on the problem to be simulated. Particularly, the problem can be simulated using Lagrange or Lagrange-Euler methods, the metal forming problem can be extended for coupling with microstructure evolution simulation, phase transformation, fracture prediction and other applications. The integration with any CAD/CAM system is performed through new module for geometry data exchange QShape that allows importing of the die geometry models even though they may have some imperfections. Automatic adaptive mesh generation works smoothly regardless appearing of possible folds. The applications of the developed system are hot and cold forging, open die forging, rolling, profile extrusion and some others.

1. MATERIAL FLOW FORMULATION

The numerical model for FEM simulation is based on flow formulation [1] where the material is considered as incompressible rigid-viscoplastic continua and elastic deformations are neglected. The system of governing equations includes

dynamic equations

$$\sigma_{ij,j} = 0 \tag{1}$$

compatibility conditions

$$\dot{\varepsilon}_{ij} = \frac{1}{2}(v_{i,j} + v_{j,i}) \tag{2}$$

constitutive equations

$$\sigma_{ij} = \frac{2}{3}\frac{\bar{\sigma}}{\dot{\bar{\varepsilon}}}\dot{\varepsilon}_{ij} \tag{3}$$

incompressibility equation

$$v_{i,i} = 0 \tag{4}$$

energy balance equation

$$\rho c\dot{T} = (k\,T_{,i})_{,i} + \beta\bar{\sigma}\dot{\bar{\varepsilon}} \tag{5}$$

and flow stress given by equation

$$\bar{\sigma} = \bar{\sigma}(\bar{\varepsilon}, \dot{\bar{\varepsilon}}, T) \tag{6}$$

where σ_{ij}, $\dot{\varepsilon}_{ij}$, v_i are the stress, strain-rate and velocity components respectively, s_{ij} is the deviatoric stress tensor, $\bar{\sigma}, \bar{\varepsilon}, \dot{\bar{\varepsilon}}$ are the effective stress, effective strain and effective strain-rate, respectively, T is the temperature, β is the heat generation efficiency which is usually assumed as $\beta = 0.9 - 0.95$, ρ is the density, c is the specific heat and k is the thermal conductivity.

Friction model proposed by Levanov et al [2] is used on the contact part of workpiece surface

$$F_t = m\frac{\bar{\sigma}}{\sqrt{3}}\left(1-\exp(-1.25\frac{\sigma_n}{\bar{\sigma}})\right) \qquad (7)$$

where m is the friction factor, σ_n is the normal contact pressure. Expression (7) can be considered as a combination of constant friction model and Coulomb friction model that inherits advantages of both ones. The second term in parenthesis takes into account the influence of normal contact pressure. For high value of contact pressure expression (7) provides approximately the same level of friction traction as constant friction model while for low contact pressure it gives friction traction that is approximately linearly dependent on normal contact stress. Experimentally determined values of m for many lubricants, materials and surface conditions in hot and cold state were experimentally obtained by Levanov and can be found in [2].

Equations (1-4) were transformed into discrete form by means of virtual work-rate principle and finite element technique. Velocity and mean stress fields are approximated by tetrahedral elements for 3D [3].

2. GEOMETRY DATA CONVERSION

The source data for simulation include:

- The geometric models of the tools (usually they are solid or surface CAD models)
- The properties of the deformed material (the flow stress and thermal properties)
- The conditions on the contact surface of the extruded material with the tools (the friction, the heat transfer coefficient, the temperature of the tools).
- The process parameters (the initial temperature of the billet, the extrusion speed, the pulling force).

When setting the source data for the simulation the problem is to transfer correctly the geometric model of the tools from CAD representation to simulation program. The simulation as any other kind of finite element analysis sets more strict requirements to the quality of the geometric model comparing to CAM where these models are usually used. Some imperfections like sharp edges, the gaps between adjacent surfaces and overlapping of the adjacent surfaces are not acceptable for simulation. In the simulation model the material slides along the surface of the tool and even small gaps or overlapping may cause the problem.

The problem of correct transfer of the geometric models from CAD to the finite element analysis is principal. In respect to the extrusion it is even more difficult because the extrusion tools can be of very complex shape. To solve this problem QuantorForm Ltd has developed special program QShape that is dedicated to import of the geometric models from any CAD system, its analysis, fixing the detected imperfections and conversion into finite element representation. The model can be in one of the following standard formats IGES, STEP or STL. Figure 1 shows some examples of the geometry of the tools as they are treated in QShape.

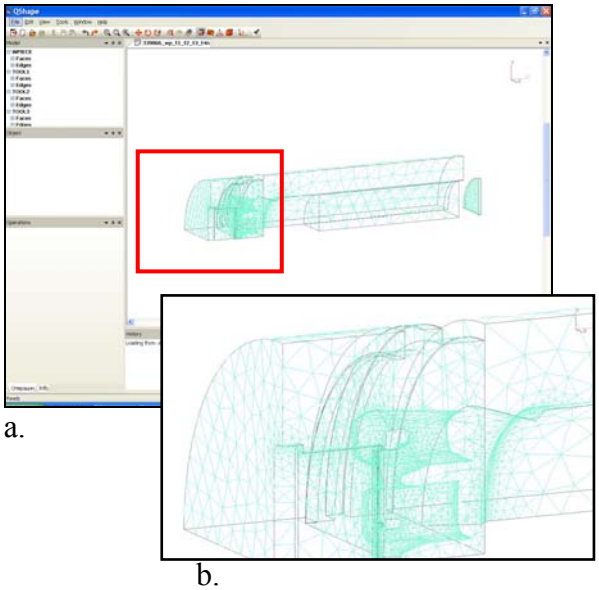

a.

b.

Figure 1. The tool geometry after its import to QShape (a) and its magnified view (b).

Besides of the import and conversion of the input geometry QShape also allows local modification of the tools without going back to CAD system that saves the time and makes the system more flexible.

3. LAGRANGE OR LAGRANGE-EULER APPROACH

Depending on the technological process the material flow simulation can be performed either in steady state or in non-steady state approach. Some processes like profile extrusion have the stage with transient material flow when it fills the container and the die and the material reaches the die orifice. At this stage the Lagrange model is to be used. The finite element mesh follows the material flow and by these means precisely traces the progress of the die filling. In extrusion of the hollow profiles the material flow separates at the "bridges" that support the mandrel and then merges again in welding zones while the Lagrange model shows the details of the material flow very clearly (Figure 2). Some defects of the tool design can be detected at this stage of the simulation. For example, if the feeder has insufficient size or inappropriate shape the simulation shows that it is not enough of the material in the welding zone and there are some voids there or the pressure there is not big enough to provide good welding conditions.

The simulation of the transient stage of the extrusion by means of the Lagrange model goes quite quickly at the beginning but then it slows down when the material reaches the die orifice. When the whole cross section of the profile is formed the Lagrange model works ineffectively. Its finite element mesh requires remeshing nearly at each time increment due to severe distortion of the elements near the small fillet radii at the entrance to the orifice. The maximum admissible size of the time increment is also very small and to get the profile of considerable length several thousands of the steps would require. Thus applicability of the Lagrange model is restricted by the moment when the tool inner space is filled. The further simulation is performed using Lagrange-Euler model.

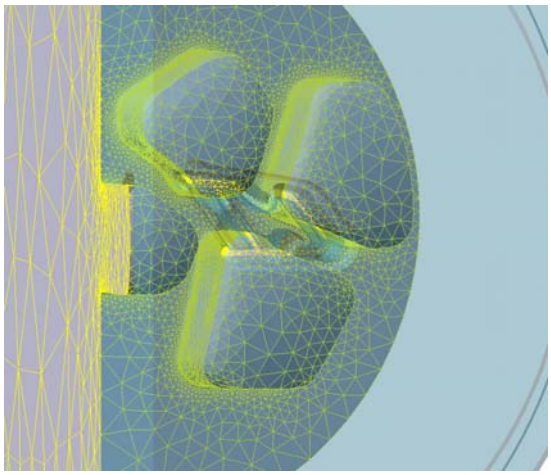

a.

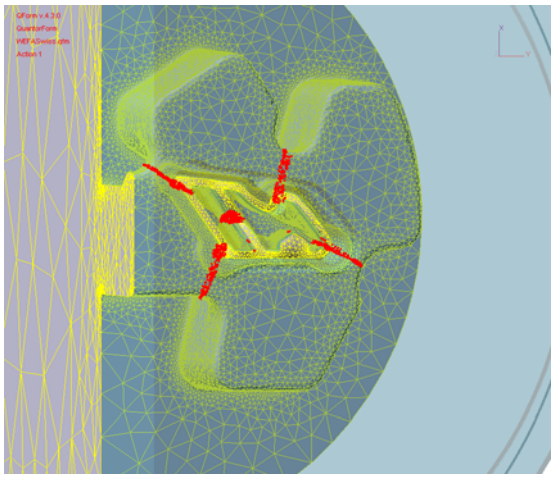

b.

Figure 2. The die filling in extrusion of the hollow profile. The materail filles the feeding chanels (a), the contact is appearing in welding zones (b).

The Lagrange-Euler model is based on the assumption that the tool is already completely filled and the domain of the material flow inside of the tool does not change. Thus the finite element mesh inside of the tool can be "released" from its tie to the material and can be tied to the space domain. This means that from now the mesh here is immovable while the material flows through it. The material leaves the Euler domain soon after it comes out of the die orifice. This approach allows do not remesh the domain inside of the tools but just to calculate the velocity in the nodes in it.

On the other hand after the orifice we have free end of the profile that increases its size very quickly. Due to specifics of the material flow the profile that leaves the orifice may bent, twist or buckle. The simulation goal is to predict this undesirable shape deterioration and to find out the ways to minimize it. The Euler model is not suitable for tracing of the profile shape evolution and the Lagrange model must be used here. To simulate this stage of the extrusion process both these models are coupled in QForm. Figure 3 shows the zones where Euler and Lagrange models are implemented and how the length of the profile increases.

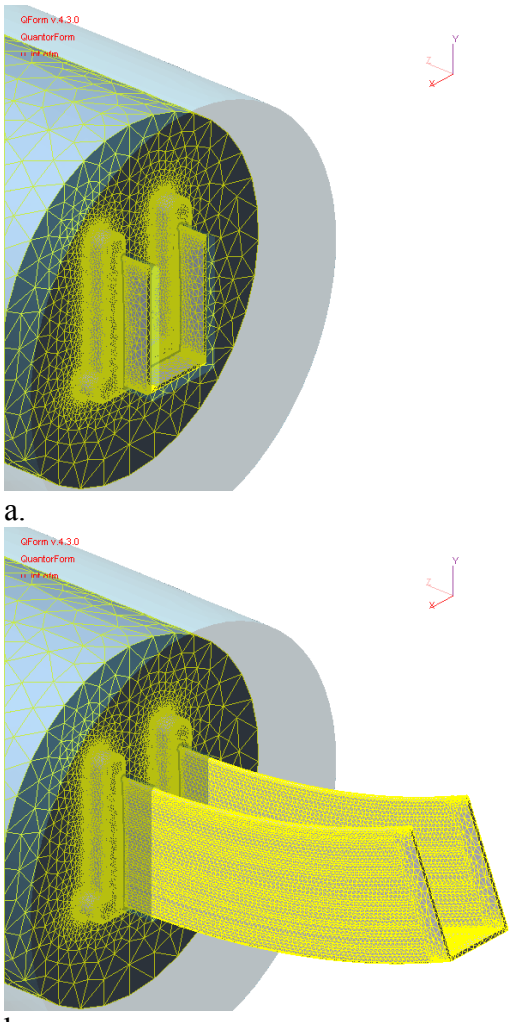

a.

b.

Figure 3. Simulation of the profile extrusion using Lagrangian-Eulerian approach: (a) beginning of calculation when the Lagrangian model is used; (b) steady-state stage of the simulation when coupled Lagrangian-Eulerian model is working.

The use of coupled Lagrange-Euler model decreases the simulation time comparing to Lagrange model many times. It is important that the simulation quality also increases. The shape of the profile is kept very accurately that allows to predict its buckling and to investigate how the process parameters (the tools shape, the friction, the temperature and the extrusion velocity) influence it.

At the third stage of the extrusion when the end of the profile is big enough it is fixed by the pulling device and the pull force is applied to eliminate its excessive bending and to provide better conditions for the process. At this stage Lagrange-Euler model is also used while some restrictions on velocity and pulling force are applied at the end of the profile.

Validation of the model was performed for the load prediction, the material flow pattern and the temperature distribution. The load was estimated using the experimental results of the 2nd Extrusion Benchmark Test [4]. Figure 4 shows the load versus time graph obtained by simulation. The experimental maximum value of the load was reported in [4] as 7.13 MN. Our simulation has shown 7.65 MN. The discrepancy about 7% can be explained by different friction conditions in the experiment and simulation.

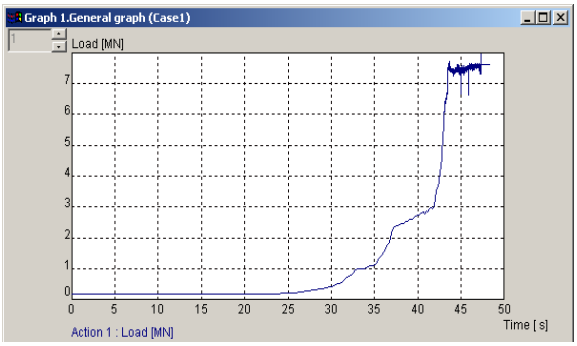

Figure 4. The extrusion load versus time calculated using Lagrange-Euler model. Experimentally measured value of the load was 7.13 MN [3].

It is very important to check the correspondence of the material flow predicted by the Lagrange-Euler model and found experimentally. This test was accomplished using the results of the cold aluminium extrusion of the rod presented in work [5]. To be as close to the experiment as possible the sticking conditions were specified on the workpiece-tool interface. As seen in Figure 5 both sets of the flow lines (longitudinal and transversal) are in good agreement with the experiment.

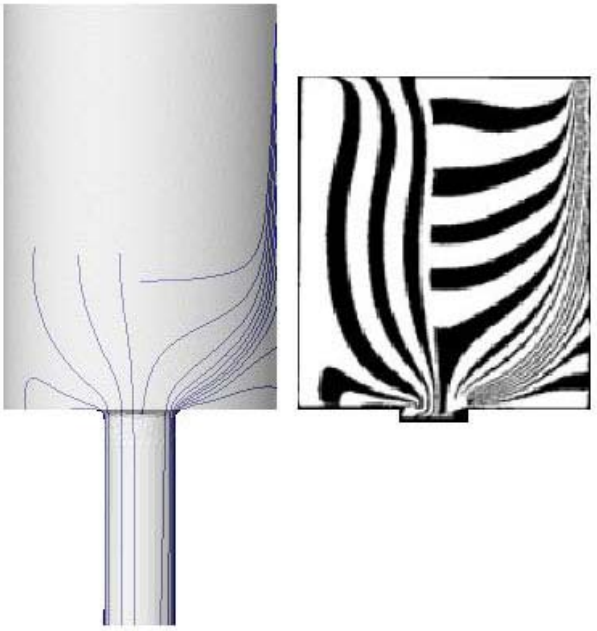

a. b.

Figure 5. The material flow pattern obtained by simulation using Lagrange-Euler model (a) and found experimentally in work [5] (b).

4. SIMULATION OF MICROSTRUCTURE EVOLUTION

QForm-Microstructure module includes a semi-empirical model based on Sellar's formulation firstly presented in [6]. The model takes into account dynamic and static recrystallisation and grain growth during the deformation operations and in the pauses when the billet is heated, cooled or heat treated.

Dynamic recrystallisation starts during the deformation process when the strain exceeds certain critical value ε_c that can be expressed as follows:

$$\varepsilon_c = a_1 * D_0^{a_2} * Z^{a_3} \qquad (8)$$

in which: D_0 is the initial grain size, Z is parameter of Zener-Holloman, $a_1...a_3$ are material dependent coefficients

The static recrystallisation can be characterized by the fraction of statically recrystallised grains X_{stat}, by the time for the 50% static recrystallisation $t_{0,5}$ and by the statically recrystallised grain size D_{stat}.

$$X_{stat} = 1 - e^{-h_1 * \left[\frac{t_p - t_o}{t_{0,5}}\right]^{h_2}} \qquad (9)$$

$$t_{0,5} = f_1 \varepsilon^{f_2} D_0^{f_3} \left[\dot{\varepsilon} * e^{\frac{Q_{st}}{RT}}\right]^{f_4} * e^{\frac{f_5}{T}} \qquad (10)$$

in which: t_p is the dead time, t_0 is the time until the beginning of the static recrystallisation, D_0 is the initial grain size before starting the static recrystallisation, Q_{st} is the activation energy for the static recrystallisation, h_1, h_2, $f_1...f_5$, $g_1...g_4$ are the material-dependent coefficients

The grain size in static recrystallisation is expressed

$$D_{stat} = g_1 \varepsilon^{g_2} D_0^{g_3} Z^{g_4} \qquad (11)$$

After a primary recrystallisation, the microstructure is not yet in the state of equilibrium. A reduction of the grain boundary energy by a decrease of the grain boundary area can be realized through the grain growth:

$$(\Delta D)^n = \lambda * t * e^{\frac{-Q_{KW}}{RT}} \qquad (12)$$

in which: t is the holding time, ΔD is the grain size increment, Q_{KW} is the activation energy for the grain growth, λ, n are the material dependent coefficients, R,T are respectively the constant and the absolute temperature.

All the material parameters in the expressions above are to be determined experimentally for every material to be simulated.

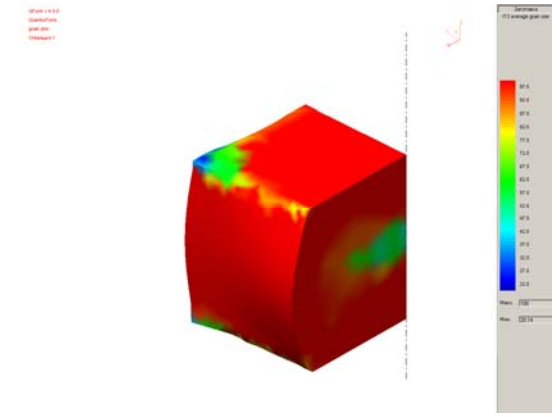

a.

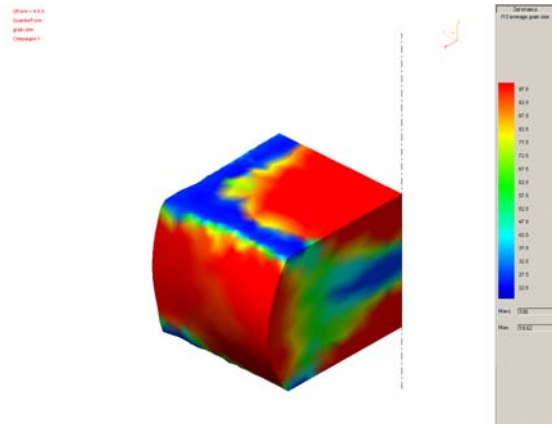

b.

Figure 6: Average grain size on the surface and in the cross sections of the upset billet.

The simulation in QForm3D Microstructure module allows predicting the average grain size and the fraction of recrystallised grains. Figure 6 shows the billet at the beginning and after the blow in open die forging of a block from Inconel 718.

The model provides the simulation of the microstructure evolution in any kind of material forming processes including closed and open die forging with subsequent heat treatment.

REFERENCES

1. Zienkiewicz O.C., Flow formulation for numerical solution of metal forming processes. In Numerical analyses of forming processes (Ed. Pittman J.F.T., Zienkiewicz O.C., Wood R.D. and Alexander J.M.), 1984, pp. 1-44.
2. Levanov A.N., Kolmogorov V.L., Burkin S.P. et al, Contact Friction in Metal Forming, Moscow, 1976 (In Russian).
3. Biba N, Stebounov S., 3D Finite Element Simulation of Material Flow, Metallurgia v. 69, 2002, No. 2, pp. FT8-FT10.
4. Extrusion Benchmark 2007. Donatti L., Tomesani L., Schikorra M., Tekkaya E.. Proceedings of the Conference Latest Advances in Extrusion Technology and Simulation in Europe. Bologna, 2007. pp. 89-95.
5. Experimental Techniques to Characterise Large Plastic Deformations in Unlubricated Hot Aliminium Extrusion. Valberg H. Proceedings of the Conference Latest Advances in Extrusion Technology and Simulation in Europe. Bologna, 2007. pp. 9-12.
6. Sellars,C.M.; Whiteman,L.A. :in Proc. Product Technology Conf. on “Controlled rolling processing of HSLA-steels”. York 1976